 MCB, vol.6, no.3, pp.175-189, 2009

Digital control circuitry of cancer cell and its apoptosis

R. M. Ardito Marretta* **and G. Barbaraci†**

Abstract: This study, through a typical aerospace systems architecture, suggests an engineering design of a human cancer cell circuitry in which a digital optimal control matrix is assigned to repair the DNA damage level and/or to trigger its apoptosis.

Here, the conceived machinery is proposed taking into account the state of the art in cancer investigation. However, it could be further generalized.

The most recent studies on cancer pathologies give a predominant role to the oncosuppressor protein p53 and its antagonist, the oncogene Mdm2.

Experimental and theoretical approaches are in agreement in deducing a "digital" response of the p53 when genomic integrity is damaged. Once DNA damage is present, the mutual influence of p53 and its antagonist, the Mdm2 oncogene, is closed in a feedback loop.

In this work, starting from these current results, a novel molecular mechanism is proposed, based on a digital optimal control law, whereby p53 and Mdm2 proteins activities can be represented by appropriate circuitry and governed by the optimal control law of digital systems.

This procedure obtains a real-time sequence evaluation of protein oscillations and an unexpected and relevant acceleration in the DNA repairing when suitable digital control matrix is implemented.

Those effects suggest interesting perspectives for future scientific investigations.

First of all, the proposed digital circuitry, receiving the p53 signal from a damaged cell, is able to repair the current level of genomic alteration. Moreover, the cell fate is newly conceived and bound by the modified pulsing mechanism of p53.

* Correspondence author. Dipartimento di Ingegneria Strutturale e Geotecnica, Università di Palermo, Edificio 8, 90128, Palermo, (Italy); Tel.: 091-6459912, Fax: 091-485439; Email: romario@unipa.it

† Department of Mechanical Engineering, University of Palermo, 90128, Palermo, (Italy)

1 Introduction

Since its discovery, the oncosuppressor p53 protein seems to play a prominent role in the evolution of a cancer cell.

Activation and high concentration of p53 are the response of the cell "system" to aberrant oncogene signals.

This protein is capable of inducing the transcription of genes in charge of the cell-cycle arrest, DNA repair and apoptosis (see Ma, Wagner, Rice, Hu, Levine and Stlovitzky (2005); Geva-Zatorsky, Rosenfeld, Itzkovitz, Milo, Sigal, Dekel, Yarnitzky, Liron, Polak, Lahav et al. (2006); Shangary and Wang (2008); Ciliberto, Novak and Tyson (2005); Zhang, Brazhnik and Tyson (2007)).

At this point, an engineering frame of mind was adopted by the present authors (whose disciplines lie inside aerospace technologies) when they faced the acknowledgement of the p53 protein inner mechanism and its role in the human single-cell architecture.

Let us view the protein p53 as a battle array in which 393 brigades (residues) form divisions (domains) having a specific biological role. Then, the functional domains of p53 are distinguished into their roles and residues; those from 1 to 42 for activation domain AD1, from 43 to 63 for another activation domain AD2, from 64 to 91 for praline-rich domain PRD, up to 364 to 393 for C-terminal basic domain BD.

An outstanding recent work (see Harms and Chen (2005)), not only confirms that the above men-

tioned domain BD of p53 is inhibitory *in vivo* but also demonstrates that activation of AD2 is required for the pro-apoptotic target gene binding protein IGFBP3. The IGFBP3 seems to play a dominant role in the apoptosis induced by N- and C- terminally truncated p53.

These conclusions seem to be related to a previous study of Bell, Klein, Muller, Hansen and Buchner (2002), in which their analysis showed that, at physiological temperatures, wild-type p53 was more than 50% unfolded with a 75% loss in DNA-binding activity. Moreover, those results found that full-length p53 contained large unstructured regions in its N- and C-terminal parts.

Although other interesting works could be considered milestones from a purely biological point of view about p53 behaviour (see Reich, Oren and Levine (1983); Ventura, Kirsch, McLaughlin, Tuveson, Grimm, Lintault, Newman, Reczek, Weissleder and Jacks (2007); Bates, Phillips, Clark, Stott, Peters, Ludwig and Vousden (1998); Bar-Or, Maya, Segel, Alon, Levine and Oren (2000)), they remain far from being used mathematically; for two reasons: first, their adopted procedures make use of chemicals, reagents and enzymes and, secondly, they become inappropriate if one decides to translate them into unsteady mathematical simulations and computational predictions.

The guidelines of the present paper are those given by Ma, Wagner, Rice, Hu, Levine and Stlovitzky (2005); Geva-Zatorsky, Rosenfeld, Itzkovitz, Milo, Sigal, Dekel, Yarnitzky, Liron, Polak, Lahav et al. (2006); Shangary and Wang (2008); Ciliberto, Novak and Tyson (2005); Zhang, Brazhnik and Tyson (2007); Bar-Or, Maya, Segel, Alon, Levine and Oren (2000); Lahav, Rosenfeld, Sigal, Geva-Zatorsky, Levine, Elowitz and Alon (2004); Loewer and Lahav (2006); Batchelor, Mock, Bhan, Loewer and Lahav (2008) in which theoretical and experimental studies about oscillations of the p53/Mdm2 feedback loop support the chance to mathematically describe this human single-cell proteins activity and their inner forms dynamics. Meanwhile, the methodological approaches, taken as frames of mind, are those of Tsourkas and Weissleder (2004); Deguchi, Ohashi and Sato (2005); Mooney (2006); Zhou, Chen and Zhang (2007).

Briefly, some of these studies come to converging conclusions, i.e., p53 can be expressed into a series of discrete pulses after DNA damage and the whole p53/Mdm2 network system is constrained by a feedback loop and theoretically expressed by a digital scheme. However, these works show differences in the analysis of results depending on the sign of the claimed feedback loops.

As a consequence, although these proposed mathematical models and experiments capture the oscillating characteristics of p53 and Mdm2, they show different and almost conflicting points of view when linked to the interpretation of results in terms of output amplitudes, frequencies, interpulses and other oscillation parameters of the p53/Mdm2 dynamic responses. In short, a negative feedback loop generates damped oscillations, while schemes such as positive feedback loops of p53 may enhance undamped dynamics.

Lahav, Rosenfeld, Sigal, Geva-Zatorsky, Levine, Elowitz and Alon (2004) confirm the p53/Mdm2 negative feedback loop oscillations once functional p53-CFP (cyan fluorescent protein) and Mdm2-YFP (yellow fluorescent protein) fusion proteins are observed through time-lapse fluorescent microscopy. After γ-irradiation at a 20min resolution during 16h of growth, these authors measured the total fluorescence in the nuclei of over 200 different cells through a movie technique. Their conclusions regarding the p53 digital behaviour consist of different fractions of cells showing zero, one, two or more pulses as a function of γ-irradiation dose; the width of each pulse was 350 ± 160min, the timing of the first pulse maximum being rather variable (360 ± 240min) after damage; the time between the maxima of two consecutive pulses is more precise, i.e., 340 ± 100min. Thus, they found that in the p53/Mdm2 feedback loop system, the number of pulses, but not the size or shape of each pulse, depends on the level of the input signal.

An important contribution for understanding the dynamics and variability of p53/Mdm2 system is given by Geva-Zatorsky, Levine, Elowitz and

Alon (2006). They evaluate the amplitude and width of each peak of nuclear Mdm2-YFP and calculate the average of these properties. Ultimately, those authors obtained prolonged undamped oscillations in the p53/Mdm2 system. The onset of oscillations was synchronized with the DNA damage signal and cells gradually lost synchrony with each other due to variations in oscillation frequencies. The characteristic oscillation frequency in each cell was found by Fourier analysis.

It should be noted that if undamped oscillations of p53 are obtained, one has to evaluate the behaviour – in the same bandwidth – of its antagonist (and its forms) for taking into account (if present) the cross-correlation factors and frequency aliasing distortion.

Batchelor, Mock, Bhan, Loewer and Lahav (2008) draw the conclusion that the p53/Mdm2 negative feedback loop is composed of interaction of two different timescales: one, a slow positive transcriptional arm and a fast negative protein-protein interaction arm. Their results show that the p53/Mdm2 feedback loop does not by itself drive sustained p53 oscillations. Thus, they identify the wild type p53-induced phosphatase 1, Wip1, as the central element mediating a second (negative) feedback loop for chaining p53 and the upstream signalling proteins.

For the present aim of this paper, two recent articles of Ciliberto, Novak and Tyson (2005); Zhang, Brazhnik and Tyson (2007) will be useful for improving a cellular circuitry which is capable of digitally processing the p53/Mdm2 system dynamics and giving a subject for discussion about its influence on apoptosis. Both these papers deal with the mechanisms for triggering p53 pulses in response to a DNA damage.

These authors elegantly showed how to obtain sustained p53 oscillations when the p53/Mdm2 negative feedback can be supplemented and integrated by a positive loop. Although negative feedback is necessary for triggering oscillations in the p53/Mdm2 system, it is not yet sufficient. In fact, if one considers a negative feedback loop with only two elements $(p53 \rightarrow Mdm2 \mapsto |p53)$, it cannot oscillate.

Moreover, in the paper of Zhang, Brazhnik and Tyson (2007), observations aimed at the employment of the p53 negative feedback loop and its observed oscillations address some important questions about the roles of positive feedback loops in generating and stabilizing oscillations and how apoptosis may be triggered by repeated pulses of p53.

It is our firm belief that understanding the prominent role of the p53/Mdm2 loop and its subsystem dynamics offers a more than promising avenue for effective cancer therapy.

Now making reference to the previous studies of Ardito Marretta and Marino (2007); Ardito Marretta, Marino and Bianchi (2008), regarding digital aerospace well-suited active control models and computer active control systems, *ad hoc* digital cellular circuitry is built up to pointwise recognize the cell damage checkpoint, the time-dependent p53 levels and the triggering of pulses. Moreover, a more complex digital cell scheme can determine different number of pulses when related to the expression of downstream genes and their evolution to give the chance – in spin-off – to assign gradients of considered species with desired levels of p53 and/or leading to cell death.

Then we propose an integration of the proposed models whatever type of feedback loop is employed. The digital control system theory, mathematically expressed in terms of state-space theory, could unify the disparate observations and offer the possibility of investigating apoptosis once the dynamics of inner protein forms is considered.

2 Adopted method

To design suitable digital circuitry for a human single-cell, we start by taking into account the protein forms of p53 (p53 mono-ubiquitinated, p53 poly-ubiquitinated and p53 total, i.e., $p53_U$, $p53_{UU}$ and $p53_{tot}$, respectively) and Mdm2 (nuclear, cytoplasmic and phosphorilated, i.e., $Mdm2_{nuc}$, $Mdm2_{cyt}$ and $Mdm2P_{cyt}$, respectively) with their time-dependency from a set of equations (see Ciliberto, Novak and Tyson (2005)). A powerful tool for resolving the problem consists of processing the set of equations in

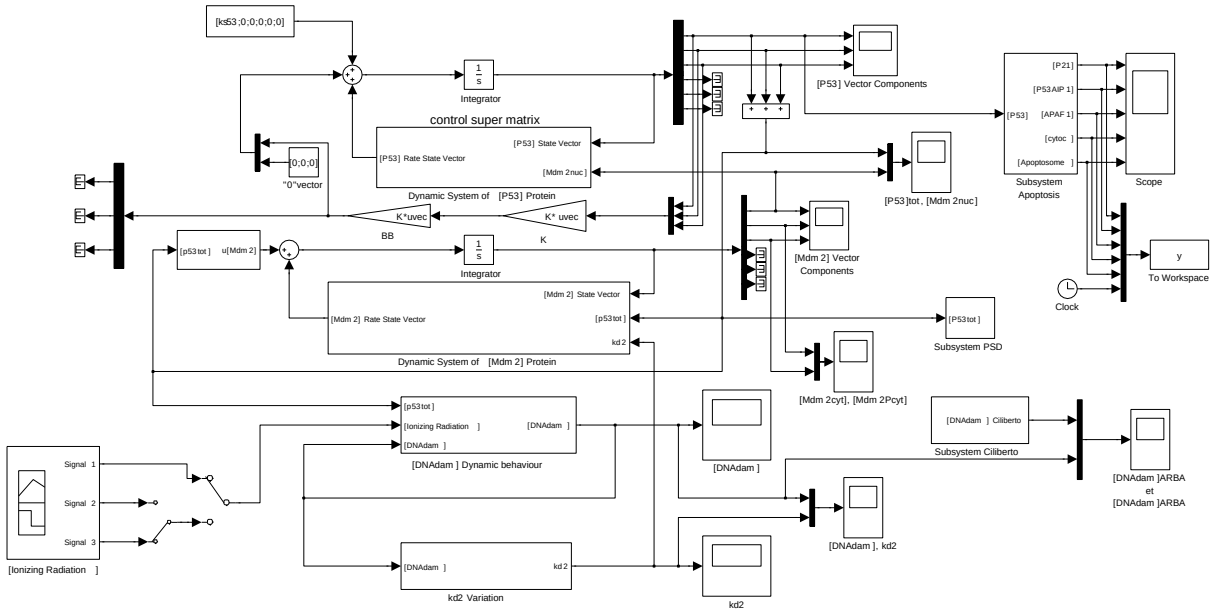

Figure 1: Human cell circuitry with control matrix

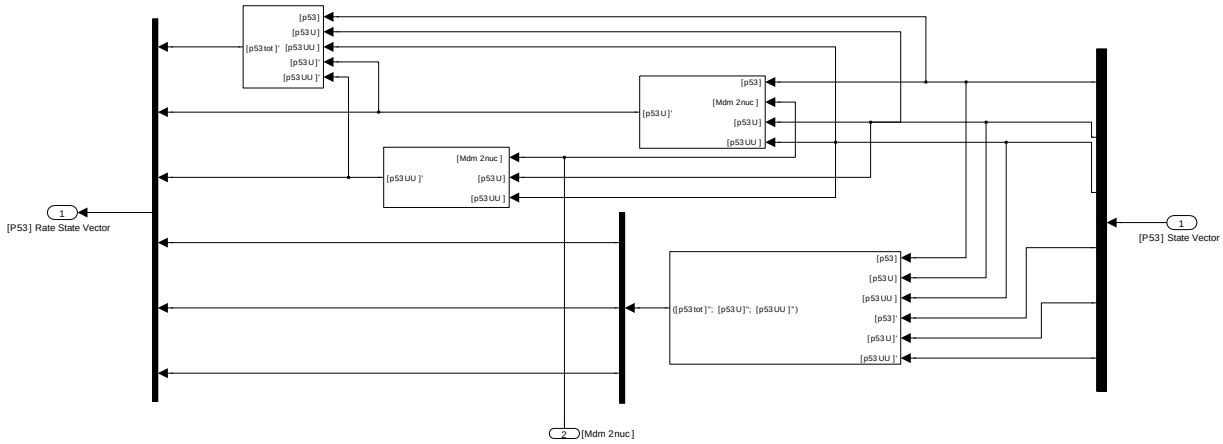

Figure 2: Cell dynamic matrix

a computational space, i.e., the *state-space* which mathematically represents all the possible conditions and combinations among the variables of the problem. Once the state-space contains the necessary equations, the numerical solution will be the task of matrix calculus. In this case, through a matrix representation in the state-space of the mutual p53 and Mdm2 dynamics, a control matrix acting in positive feedback can be obtained and processed.

Control theory is widely employed in many engineering designs and several digital control strategies are currently applied to suppress or amplify instabilities and/or margins of safety. For digitally design of such control computer-aided systems, devoted algorithms must be developed and processed in appropriate circuitries. Similarly to typical digital control system design, a convenient set of mathematical equations may be available for processing the biological system parameters and their mutual influences. For the single cell circuitry design, we digitally transform the math-

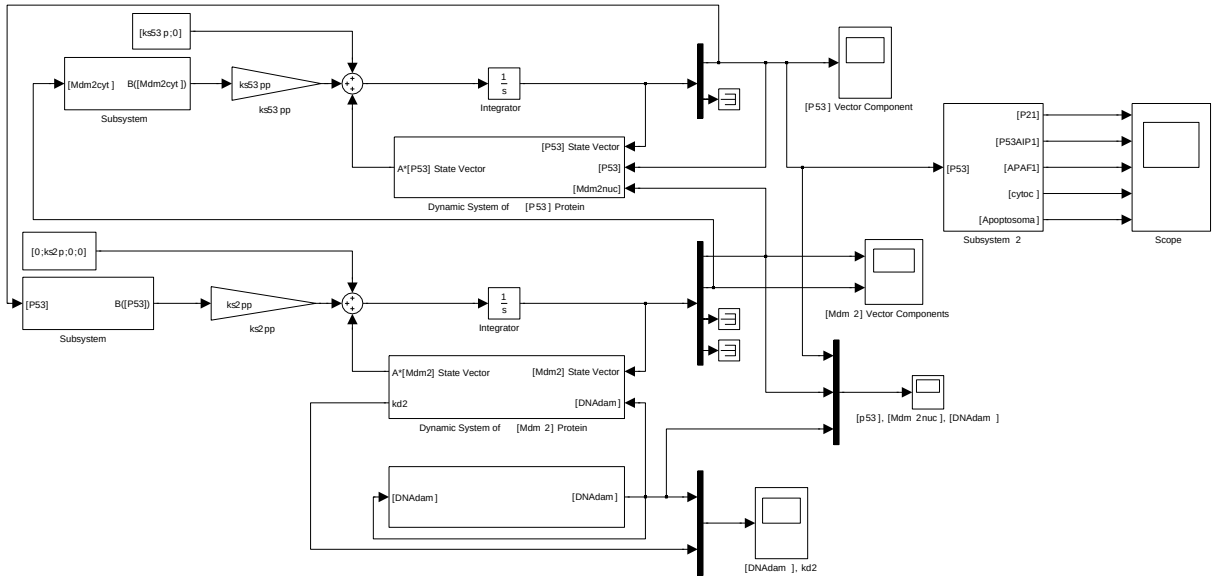

Figure 3: Cell digital circuitry (model #1 Zhang, Brazhnik and Tyson)

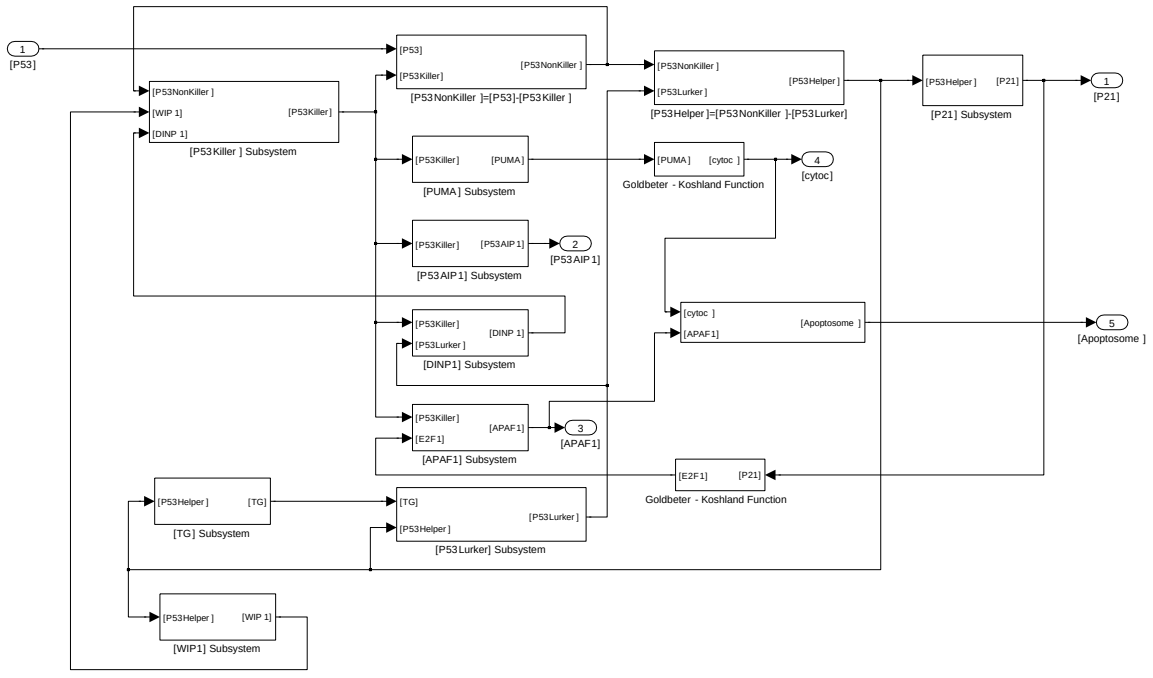

Figure 4: Apoptosis cell circuitry close-up

ematical model proposed by Ciliberto, Novak and Tyson (2005) (see figs 1 and 2) and the model #1 of those employed by Zhang, Brazhnik and Tyson (2007) (see fig. 3).

Also, we digitally connect the control circuitries obtained from those models with a wiring diagram of apoptosis (fig. 4), as given by Zhang, Brazhnik and Tyson (2007).

Making use of *Simulink*© software to assemble the wiring digital platform, the single-cell digital circuitries of the two models (see tables 1 and 3 of Ciliberto, Novak and Tyson (2005); and model #1 of those employed by Zhang, Brazhnik and Tyson (2007), respectively) have been designed. Further, one must note that the control matrix is only applicable to the model of Ciliberto, Novak and Tyson (2005) and not to the employed model of Zhang, Brazhnik and Tyson (2007) because in the former the p53 influence on the DNA damage is mathematically connected, while, in the latter, this does not occur.

The reliability of the digital circuitry design is ensured in two different ways: in the first model – switching "off" the digital control matrix block (see fig. 1) – we coherently obtain the same results as Ciliberto, Novak and Tyson (2005) for the p53/Mdm2 dynamics when the same amount of DNA damage is imposed (see fig. 5). It is worth noting the simulated results are in almost perfect accordance not only with the numerical results of Ciliberto, Novak and Tyson (2005) but also with experimental data of Bar-Or, Maya, Segel, Alon, Levine and Oren (2000) and Ma, Wagner, Rice, Hu, Levine and Stlovitzky (2005) moreover, the other digital circuitry faithfully repeats the p53/Mdm2 evolution of the model #1 of Zhang, Brazhnik and Tyson (2007), as shown in fig. 6. These two numerical and biological "checkpoints" shown in figs 5 and 6 seem to be necessary to justify the utility of the present (digital) approach.

Now, it should be noted that, in state-space theory, an applied digital wiring control scheme – based on the extended form of ODEs (ordinary differential equations) employed by Ciliberto, Novak and Tyson (2005); Zhang, Brazhnik and Tyson (2007) – should be not applicable in the state-space itself. This is due to the presence in the state-vector – as components – of both the p53 forms and its derivatives. To overcome this inconvenience, one must consider in the proposed mathematical models (see Ciliberto, Novak and Tyson (2005); Zhang, Brazhnik and Tyson (2007)) the absence of relationships among the first-derivatives on the right-hand side of the equations and those put on the left-hand side. Let us now describe in detail the procedures employed.

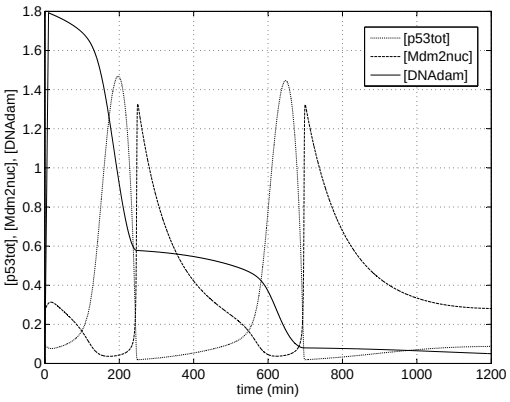

Figure 5: p53/Mdm2 pulses with DNA damage (Ciliberto, Novak and Tyson)

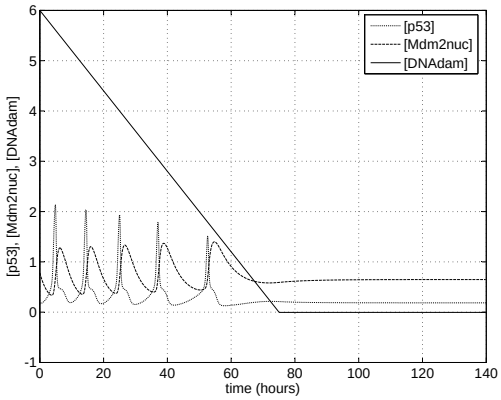

Figure 6: p53/Mdm2 pulses with DNA damage (model #1 Zhang, Brazhnik and Tyson)

3 Optimal digital control

Before of describing the advantages of applying the digital optimal control matrix, one has also to check the reliability of the built up digital cir-

cuitries according to the mathematical aspects of the adopted models and their translation into the state-space theory.

A) Model of Ciliberto, Novak and Tyson – Taking into account their system of non-linear/first order differential equations (ODEs), one can describe both p53 and Mdm2 dynamics as well as the evolution of their forms. This mathematical approach is capable of deducing the mutual influence among these concentrations. The digital circuitry shall be able to reproduce the experimental basis of this model, i.e.:

a) Mdm2 and p53 are mainly degraded in the cell nucleus; b) Mdm2 is the activator of a reaction for degrading p53 in a ubiquitin-manner; c) Mdm2 attaches only two ubiquitins of p53 ($p53_U$ and $p53_{UU}$); d) three forms of p53 ($p53_U$, $p53_{UU}$, and $p53_{tot}$) induce transcription of Mdm2 in nonphosphorilated and cytoplasmic forms; e) for translocating into the nucleus, $Mdm2_{cyt}$ needs to be phosphorilated ($Mdm2_{cyt} \rightarrow Mdm2P_{cyt}$); f) the phosphorilated cytoplasmic $Mdm2P_{cyt}$ moves freely into and out of the nucleus; g) phosphorilation of $Mdm2_{cyt}$ is inhibited by $p53_{tot}$ in looping.

In the present study, to achieve the optimal control scheme – based on an *LQR*-type (*Linear Quadratic Regulator*) kernel – a suitable manipulation of the previous set of ODEs has been done for writing and using them from the extended form into the state-space representation.

Following this procedure, a dynamic matrix representation of the p53/Mdm2 system is obtained in which the time-dependent and mutual influence of these proteins can be fully described. From now on, the inner mechanisms of degradation of forms of cell proteins and/or phosphorilation are marginally mentioned, the purpose of the present work being a global mathematical procedure to design a cellular circuitry and the post-processing of the output.

In agreement with to but differently from Ciliberto, Novak and Tyson (2005), in the present procedure, a non linear ODEs system has been employed to write the set of equations with respect to the p53 protein and not to the total p53. In more detail, the state-vector for p53 and its concentrations shall be

$$x(t) \triangleq \left[[p53]\,[p53_U]\,[p53_{UU}]\,[\dot{p53}]\,[\dot{p53}_U]\,[\dot{p53}_U] \right]^T$$

where the overdot represents the time-derivative and the subscripts U, UU identify the first-, the poly-ubiquitin protein forms, respectively; while the vector

$$\underline{b} = \begin{bmatrix} k_{s53} & 0 & 0 & 0 & 0 & 0 \end{bmatrix}^T$$

contains the coefficient of Ciliberto, Novak and Tyson (2005). The vector $\underline{b}$ is defined once the state-space representation is implemented for describing the input-state relationships.

We consider the level of $[Mdm2_{nuc}(t)]$ as a time variable and a matrix $\underline{\underline{P}}$ for the dynamic activity of p53 (time-variant). Mdm2 dynamics can be expressed by a vector in the state-space.

Once the proposed state-space representation gives the same results as the model of Ciliberto, Novak and Tyson (2005), the digital optimal control law has been implemented and based on the assumption that the matrix is such that $[Mdm2_{nuc}]$ is equal to a constant. Then, the compact expression

$$\mathbf{P} = \left\{ \underline{\underline{P_{ij}}}; \quad i,j = 1,2,3 \; so\; that \; p_{ij} \in \Re \right\}$$

represents the time-invariant dynamic supermatrix. Using the digital scheme, several simulations have been performed and they allowed the identification of the constant value of $[Mdm2_{nuc}]$ equal to 0.1 in such a way as to obtain a rate of DNA repair much more quickly than was obtained by Ciliberto, Novak and Tyson (2007).

B) Model #1 of Zhang, Brazhnik and Tyson – At first, the question formulated in this work seems to be appropriate, i.e., is a negative feedback loop (p53 upregulates Mdm2, which deactivates p53) sufficient to explain the observed oscillation?

In fact, from a purely mathematical point of view, the feedback becomes positive if it is considered as a *part* of a complete typical digital system. Instead, if one looks at the single state-vector quantities (in feedback) containing all the forms of p53, then the feedback loop becomes "hybrid" (positive - negative) in itself, because any element

of the control matrix has opposite sign with each other. In a schematic representation, one has the control matrix as follows

$$\underline{\underline{K}} = \begin{bmatrix} +k_{11} & -k_{12} & +k_{13} \\ \vdots & +k_{22} & -k_{23} \\ sym & \cdots & +k_{33} \end{bmatrix}; \; k_{ij} > 0$$

The optimal control matrix is derived from the stabilizing solution of the Riccati equation as a function of the dynamic matrix of the protein p53 whose elements are the reaction coefficients of Ciliberto, Novak and Tyson (2005). The above k_{ij} matrix elements are, in turn, functions of those coefficients.

In the model #1 of Zhang, Brazhnik and Tyson (2007), Mdm2 activates p53. Combined with p53-induced Mdm2 transcription, Mdm2 thereby enhances its own synthesis. The values of stable steady state concentrations are obtained once the level of the DNA damage is set equal to zero. When this level is different from zero, the degradation of nuclear Mdm2 increases and its concentration begins to fall. The interesting result of this model is that if the damage level is quickly repaired, the p53/Mdm2 control system develops a single-pulse response to repair the DNA damage itself. The second pulse occurs if the level of the DNA damage is relatively high. Also in this case, the designed digital circuitry faithfully reproduces the results as shown in fig. 6.

C) Apoptosis – Zhang, Brazhnik and Tyson (2007) show a wiring diagram of apoptosis and apply it to their model #1 (see fig. 2 of Zhang, Brazhnik and Tyson (2007)). Although the above mentioned models (Ciliberto, Novak and Tyson (2005); Zhang, Brazhnik and Tyson (2007)) give different evolutions of the DNA damage repairing, digital control theory in state-space can unify these models on the basis of the developed control matrix. Indeed, a well-suited optimal control law allows any DNA damage evolution to be assigned to the realized human single-cell circuitry. Then, we take into account the DNA damage level and shape proposed by Zhang, Brazhnik and Tyson (2007) applied to the model of Ciliberto, Novak and Tyson (2005) once it is connected to a wiring diagram of apoptosis (see figs 1 and 4).

4 Results and discussions

Once the reliability of the adopted cellular digital circuitries has been tested apart from the sign of the feedback loop, thanks also to the dynamic control matrix, we study its effects on the proteins systems of the p53/Mdm2 network in presence of a DNA damage.

Here, we consider the running digital control process for the previous selected models of Ciliberto, Novak and Tyson (2005); Zhang, Brazhnik and Tyson (2007) and evaluate the p53 dynamics in interaction with the other protein parameters and the DNA damage levels. All the recursive routines and circuitries were processed using *Matlab*/*Simulink* platforms at the Department of Mechanical Engineering – University of Bath (UK) – under the supervision of doctor Michael Carley.

A) Model of Ciliberto, Novak and Tyson – Looking at the simulation output when the digital control matrix is switched "on", it has been roughly noted that the $p53_{tot}$ and $Mdm2_{nuc}$ levels increase throughout the same timescale (see fig. 7) when compared to the results having the digital control matrix switched "off"; since high levels of $p53_{tot}$ involve a decrease in the DNA damage, we now switch the [$Mdm2_{nuc}$] level to its lowest value in such a way as to obtain a positive feedback loop according to the digital control theory rules.

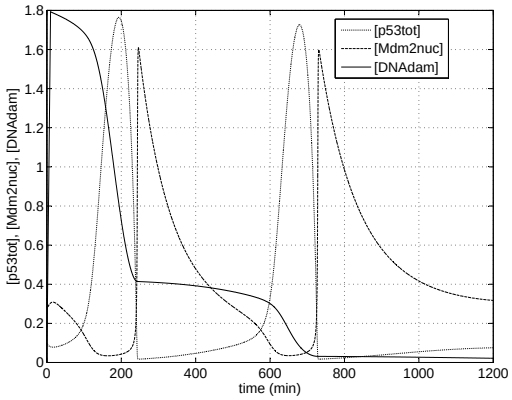

Figure 7: p53/Mdm2 pulses with DNA damage (controlled)

Surprisingly, the results change deeply. Digital optimal control is then able to realize remarkable

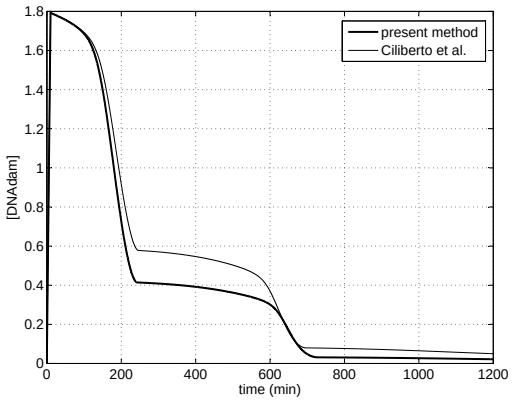

Figure 8: DNA repair comparison

effects: first of all, a DNA damage repair speed faster than 50% (see fig. 8) and – in cascade – a relevant variation of p53/Mdm2$_{nuc}$ dynamics. From the comparison between figures 5 and 7, one may deduce that the oscillation parameters of p53/Mdm2 have been modified in terms of amplitudes (higher concentrations) and interpulse (time-shift in the second pulse of about 40min). The initial conditions of Ciliberto, Novak and Tyson (2005) being equal, the faster rate of DNA damage repair can strongly affect the response of the whole p53/Mdm2$_{nuc}$ dynamics. Moreover, the optimal control matrix is able to output sustained amplitudes of both p53 and Mdm2$_{nuc}$ values.

The dual action of the control matrix has different damping effects: these are more evident for the second pulse of p53 and almost irrelevant for Mdm2. This different behaviour in the second pulse is linked to the local gradient of the DNA damage repair pathway; while in the first pulse, the difference – between the uncontrolled and controlled models – of the DNA damage levels is very high, the local pathways and then the gradients are quite superimposable up to 220min. When the second pulse triggers, the DNA local damage levels are totally different in shape (gradient) and amplitudes. In the uncontrolled digital system, the gradient is confined inside a range of 80min, while in the controlled one, the range becomes wider up to 120min. In any case, as regards the p53/Mdm2$_{nuc}$ system, the action of the control matrix implies an overall effect, i.e., an amplifying of concentrations scattered along the same timescale. Also, the global interpulse of the p53/Mdm2 network is shifted; from a comparison between figures 5 and 7, one can deduce that its first pulse triggers at the same time interval (200÷240min); while, in the digital control system, the second pulse occurs after a delay of 600+48min. Both the uncontrolled and controlled digital circuitries show in-phase oscillations of the single protein forms, the frequency of the [p53$_{tot}$/Mdm2$_{nuc}$]$_{uncontr}$ system being equal to 3.78×10^{-5}2.5 $\times 10^{-3}$Hz and 3.3×10^{-5}Hz for [p53$_{tot}$/Mdm2$_{nuc}$]$_{contr}$ network.

The use of appropriate cell digital machinery reveals interesting perspectives for future biology spin-off. Two of them seem to be easily demonstrated, i.e., robustness and generalization. Accuracy of results, freedom in choosing any other cell proteins forms, genotypes and/or target genes, circuitry components manipulations and low computational resources yield reason enough for these conclusions.

B) Model #1 of Zhang, Brazhnik and Tyson – As mentioned before, this model has been converted into a digital platform circuitry for two reasons: one, to check the reliability of the cell digital machinery and, second, for the proposed apoptosis wiring diagram shown and linked by those authors to this model. As mentioned before – in the light of the interchangeability of the previous digital control matrix – we adopt this model and its protein forms to analyse the response of the system when an apoptosis wiring diagram is considered. In this model, Mdm2 activates p53 and, in positive feedback, p53 and Mdm2$_{cyt}$ abruptly increase. At this point, an increasing quantity of Mdm2 migrates into the nucleus so giving degradation of p53 and a decrease in its level. As a consequence, the Mdm2 rate decreases and, accordingly, the Mdm2$_{nuc}$ level drops (see fig. 6). In this model, the initial DNA damage is repaired at a constant rate. When a wiring diagram of apoptosis is connected to this model, those authors define three forms of p53 (*helper*, *killer* and *lurker*) and follow the evolution of these forms to elegantly deduce and propose a digital apoptosis mechanism by numbering the p53 pulses. In agreement with

to but differently from those authors, we link their apoptosis wiring diagram – digitally converted – to cell digital circuitry having a digital control matrix (see fig. 1).

C) Apoptosis – the decision on cell fate is now conceived and bound through the modified pulsing mechanism of p53 and other considered species when the cellular digital optimal control system is applied to an apoptosis wiring diagram (see figs 1, 4 and 9). Following Zhang, Brazhnik and Tyson (2007), we take into account their apoptotic model (see table 5 of their mentioned work). In sequence, switching "on" and "off" the cell digital connection of the control matrix, the controlled ("on") and uncontrolled feedback ("off") networks (see fig. 9) give results concerning the time evolution of the apoptotic species (cyclin-dependent kinase inhibitor, p21; p53-regulated apoptosis-inducing protein 1, p53AIP1; apoptotic protease activating factor 1, APAF1; and target gene "cytoc" as a functional of APAF1 in apoptosome expression), the value of apoptosome parameter (expressed by the Heaviside function) being equal to 1 for matching (or not) the cell death. The species dynamics comparison – both in the uncontrolled and controlled networks – sketched in fig. 10 show remarkable information. First of all, instabilities of apoptotic species vanish in the digital control system and, in sequence, variations of cell death parameter in terms of timescale and triggering occur. In the uncontrolled system, the cell fate triggers at 124.61min and goes on for 32.3min, while in the digital controlled network cell fate triggers at 115.3min and remains for 27.7min. Moreover, interesting topics of discussion can be derived from the previous results when they are sketched all at once on the same timescale (see figs 11 and 12). Both the uncontrolled and controlled systems (although with different triggering and time range) show apoptotic phase just in correspondence with the inflexion point of the considered species pathways. A possible and common (for both the networks) unification could be mathematically expressed: cell death triggers when the local gradients of the species (p21 being equal to zero) reach their maximum values at the same instant; apoptotic phase remains until all the considered species match their numerical maximum values; then p21 triggers. Once the local gradient of p21 reaches its transient maximum value, the cell death phase ends.

To sum up, we have reason to believe that the evidence of designing a cell digital platform could be useful and representative in studying p53/Mdm2 evolution in a cancer cell and its fate. This is a first step. Limitations of the current digital design can be found in its application to a single-cell and the hypothesis of the considered number of apoptotic species (one has to remember that only some cases of Zhang, Brazhnik and Tyson (2007) match cell death).

Nevertheless, those limitations can become future qualities when the proposed digital cell circuitry is enhanced for multi-cellular systems and for suitable feedback of the ionizing radiation signal, which will be studied in future work.

5 Outcome reproducibility

Once the initial conditions of stable steady-state are considered (see table 1), a digital control circuitry design can be performed through the protein [p53] state-space representation (or the equivalent [Mdm2] in feedback), i.e.:

$$\dot{x}(t) = \underline{\underline{P}}([Mdm2_{nuc}(t)])\, x(t) + b \tag{1}$$

$$z(t) = \Big[[Mdm2_{nuc}]\ [Mdm2_{cyt}]\ [Mdm2P_{cyt}]\ [\dot{Mdm2}_{nuc}]\ [\dot{Mdm2}_{cyt}]\ [\dot{Mdm2P}_{cyt}] \Big]^T \tag{2}$$

$$\dot{z}(t) = \underline{\underline{M}}([p53_{tot}(t)], k_{d2}(t)) + c([p53_{tot}(t)]) \tag{3}$$

$$c = [0\, f([p53_{tot}(t)])\, 0\, 0\, 0]^T \tag{4}$$

where $[Mdm2_{nuc}(t)]$ defines the time-dependent oncogene concentration rate in nuclear form during the DNA repairing action; while, $[Mdm2_{cyt}]$ and $[Mdm2P_{cyt}]$ are the time-dependent oncogene concentration rates in cytoplasmic and phosphorilated forms, respectively; $k_{d2}(t)$ is the rate constant for degradation of $[Mdm2_{nuc}(t)]$; the time-dependent expression $f([p53_{tot}(t)])$ represents the Hill function.

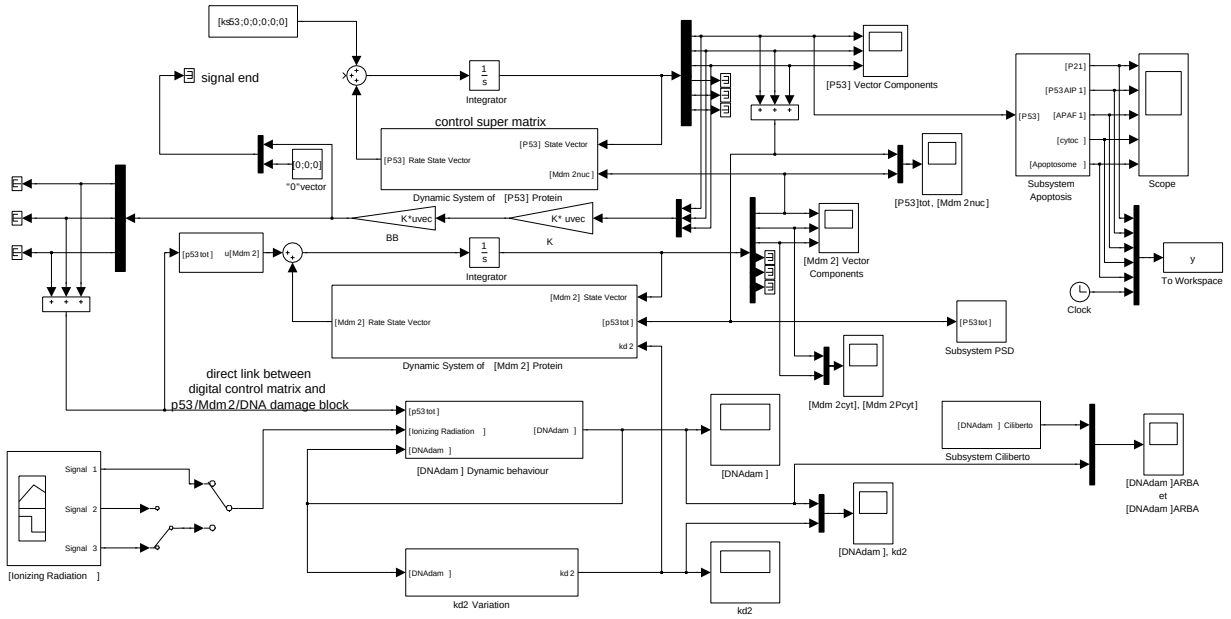

Figure 9: Human cell circuitry control matrix switched "off"

One has to note all the blacked quantities above mentioned are denoting time varying scalar quantities. Meanwhile, $\underline{\underline{P}}$ and $\underline{\underline{M}}$ identify the dynamic matrices for the trascription factor p53 and the Mdm2 oncogene, respectively. They are obtained once a state-space representation model has been carried out by the extended expression of the ODEs employed by Ciliberto, Novak and Tyson (2005).

The subscripts *nuc*, *cyt* and *Pcyt* identify nuclear, cytoplasmic and phosphorilated cytoplasmic protein forms, respectively; while the vector (4) contains the known Hill function f previously used by Ciliberto, Novak and Tyson (2005) (for the coefficients, see tables 1-2).

More precisely, some auxiliary matrices have been employed as follows:

$$\underline{\underline{K}} = LQR\left(\underline{\underline{P}}, \underline{\underline{BB}}, \underline{\underline{Q}}, \underline{\underline{R}},\right) \tag{5}$$

where $\underline{\underline{K}}$ is the digital optimal control law matrix obtained by resolving the Riccati's equation, $\underline{\underline{BB}}$ the input-state transition matrix, while the positive definite matrices $\underline{\underline{Q}}$ and $\underline{\underline{R}}$ are defined in such a way their diagonal contains the setting values to obtain suitable control law for a desired protein forms dynamics. The pre-multiplying factors of the matrices $\underline{\underline{Q}}$ and $\underline{\underline{R}}$ have been imposed in such a way that the pathways of the components of the state-vectors $x(t)$, $z(t)$and the DNA damage are quite similar to those of Ciliberto, Novak and Tyson (2005), while the optimal control matrix has to accomplish the task to accelerate the DNA repair process according to the equation:

$$\begin{aligned}\frac{d\left[DNA_{dam}\right]}{dt} &= kDNA[IR] \\ &- k_d DNA\left[p53_{tot}\right]\frac{\left[DNA_{dam}\right]}{J_{DNA}+\left[DNA_{dam}\right]}\end{aligned} \tag{6}$$

in which IR represents the functional of the imposed radiation dose; while $kDNA$, k_dDNA, $[DNA_{dam}]$, J_{DNA} represent the (direct) rate constant linked to ionizing radiation, the direct constant rate linking DNA damage to the rate of transcription factor $p53_{tot}$, the amount of damaged DNA and the Michaelis constant of $p53_{tot}$-dependent DNA damage, respectively.

The system of differential equations obtained must be processed and resolved, i.e.:

$$\begin{cases}\underline{\underline{P}}^T\underline{\underline{S}} + \underline{\underline{SP}} - \left(\underline{\underline{SBB}}\right)\underline{\underline{R}}^{-1}\left(\underline{\underline{BB}}^T\right) + \underline{\underline{Q}} = 0 \\ \underline{\underline{K}} \equiv optimal\ control\ law\ = \underline{\underline{R}}^{-1}\left(\underline{\underline{BB}}^T\underline{\underline{S}}\right)\end{cases} \tag{7}$$

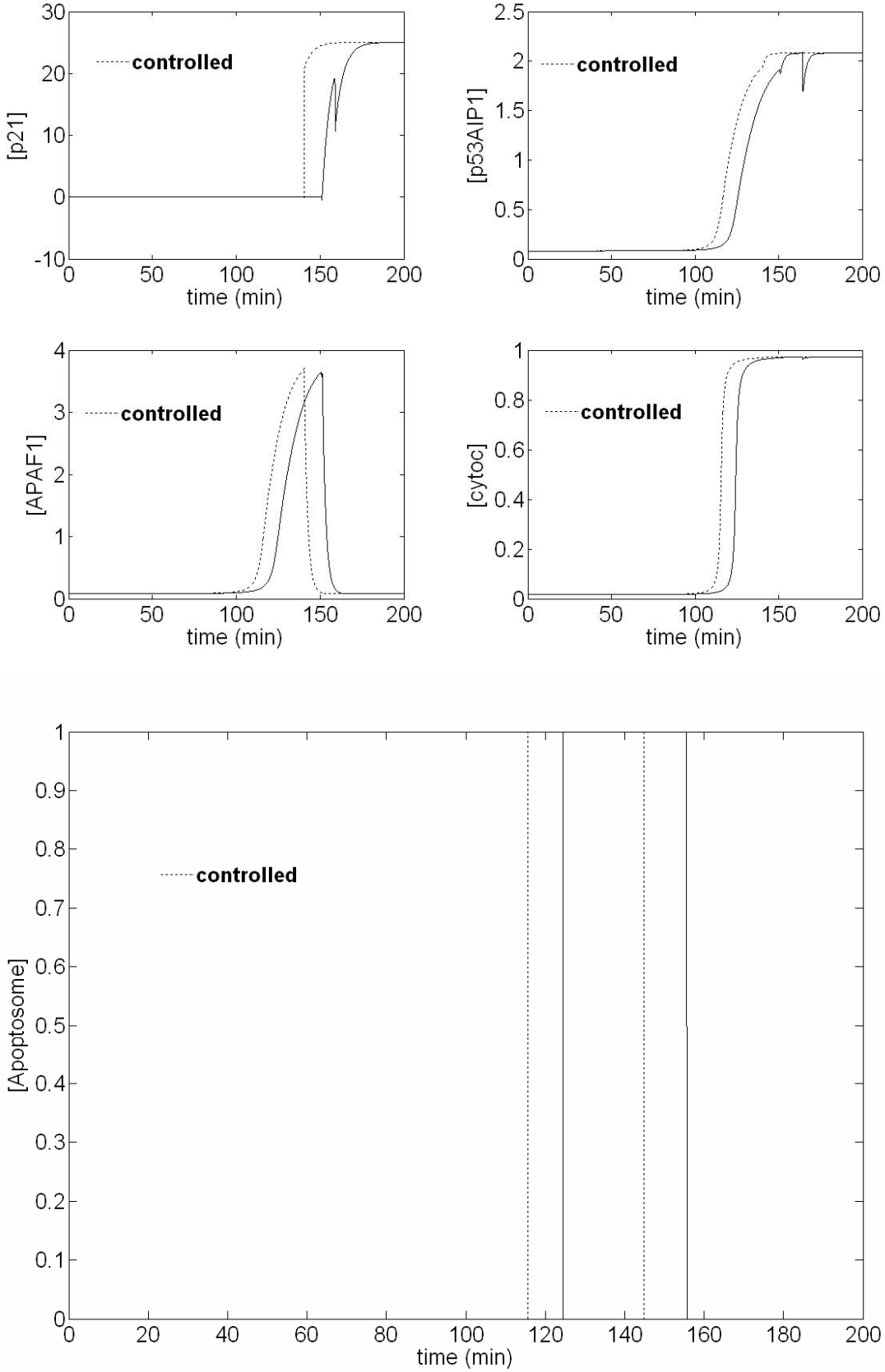

Figure 10: Species evolution in apoptosis comparison (uncontrolled/controlled)

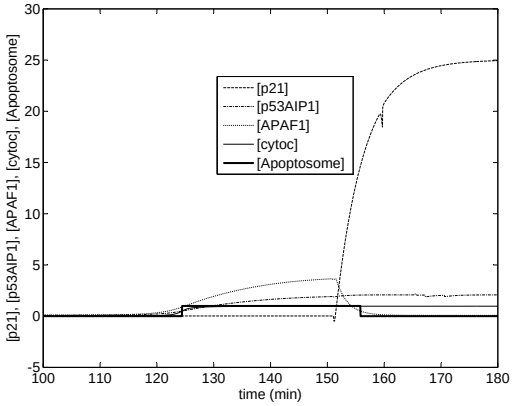

Figure 11: All at once species time history in apoptosis (uncontrolled)

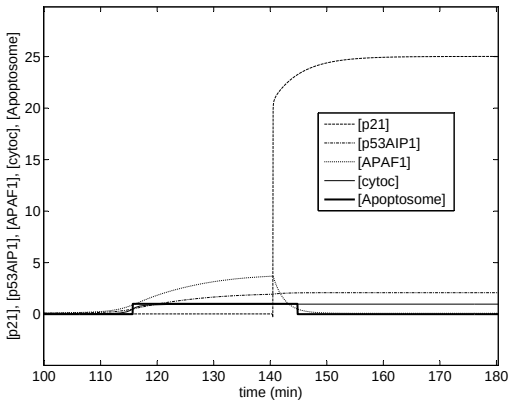

Figure 12: All at once species time history in apoptosis (controlled)

Table 1: Parameters for the p53/Mdm2 network model

Parameters	Description	Values
f	Hill function	
$q_{ij} \in \underline{\underline{Q}}$	Bryson rule matrix diagonal elements (LQR)	1min^{-1}
$r_{ij} \in \underline{\underline{R}}$	Bryson rule matrix diagonal elements (LQR)	0.5min^{-1}
k_{s53}	Rate of overexpressed $p53_{tot}$	0.055min^{-1}
k_{d53}	Rate of $p53_{UU}$ degradation	8min^{-1}
k'_{d53}	Rate of $p53_{tot}$ degradation	0.0055min^{-1}
k_f	Rate of $Mdm2_{nuc}$-dependent $p53_U$ degradation	8.8min^{-1}
k_r	Translation rate of $p53_{UU}$	2.5min^{-1}
k_{DNA}	Rate IR-dependent DNA damage	0.18min^{-1}
k_{dDNA}	Rate of $p53_{tot}$ degradation-dependent DNA damage	0.017min^{-1}
IR	Ionizing Radiation	
J_{DNA}	State variable in Hill function for DNA repair	1
$ampl$	IR dose amplitude unit	1

Table 2: Optimal control matrix coefficients

Matrix elements	Description	Constant
k_{11}	Digital optimal control matrix element	0.0023min^{-1}
$k_{12} = k_{21}$	"	0.0017min^{-1}
$k_{13} = k_{31}$	"	0.0004min^{-1}
k_{22}	"	0.0015min^{-1}
$k_{23} = k_{32}$	"	0.0004min^{-1}
k_{33}	"	0.0001min^{-1}

from the first equation of the above system, one obtains the Riccati stabilizing solution $\underline{\underline{S}}$, and the second equation is then solved.

The optimal control matrix terms being a function of the following parameters

$$\begin{cases} \underline{\underline{K}} = k_{ij} \in \Re / \\ \qquad k_{ij} = f\left(q_{ij}, r_{ij}, [Mdm2_{nuc}], k_f, k'_{d53}, k_{d53}, k_r\right) \\ [Mdm2_{nuc}] = const \\ q_{ij} \in \underline{\underline{Q}} \\ r_{ij} \in \underline{\underline{R}} \end{cases} \tag{8}$$

where k_f, k'_{d53}, k_{d53} and k_r are the translation rates of $[Mdm2_{nuc}]$, $[p53_{tot}]$, $[p53_{UU}]$ and the translation rate of $[p53_{UU}]$-dependent $[p53_U]$, respectively.

Easy mathematical manipulation of the equation of p53 yields:

$$\frac{d}{dt}[p53_{tot}] = \frac{d}{dt}[p53] + \frac{d}{dt}[p53_U] + \frac{d}{dt}[p53_{UU}] \tag{9}$$

and then one obtains:

$$\begin{aligned} &\frac{d}{dt}[p53] = \\ &-k'_{d53}[p53] - \left(k'_{d53}[p53_U] + \frac{d}{dt}[p53_U]\right) \\ &\qquad - \left(\left(k'_{d53} + k_{d53}\right)[p53_{UU}] + \frac{d}{dt}[p53_{UU}]\right) \end{aligned}$$

$$\begin{aligned} &\frac{d}{dt}[p53_U] = k_f[Mdm2_{nuc}][p53] \\ &-\left(k'_{d53} + k_r + k_f[Mdm2_{nuc}]\right)[p53_U] + k_r[p53_{UU}] \end{aligned}$$

$$\begin{aligned} &\frac{d}{dt}[p53_{UU}] = k_f[Mdm2_{nuc}][p53_U] \\ &\qquad - \left(k'_{d53} + k_{d53} + k_r\right)[p53_{UU}] \end{aligned} \tag{10}$$

Now, if the optimal control law is applied, further terms belonging to the matrix $\underline{\underline{K}}$ must be added, and then the extended form of the final system of equations is obtained. Rearranging the system (10), one comes to:

$$\begin{aligned} \frac{d}{dt}[p53] = &-\left(k'_{d53} + k_f[Mdm2_{nuc}]\right)[p53] \\ &+ k_r[p53_U] + k_{s53} + \sum_{n=1}^{3} k_{1,n} x_{n,1} \end{aligned}$$

$$\begin{aligned} &\frac{d}{dt}[p53_U] = k_f[Mdm2_{nuc}][p53] \\ &-\left(k'_{d53} + k_r + k_f[Mdm2_{nuc}]\right)[p53_U] \\ &\qquad + k_r[p53_{UU}] + \sum_{n=1}^{3} k_{2,n} x_{n,1} \end{aligned} \tag{11}$$

$$\begin{aligned} \frac{d}{dt}[p53_{UU}] = &\, k_f[Mdm2_{nuc}][p53_U] \\ &- \left(k'_{d53} + k_{d53} + k_r\right)[p53_{UU}] + \sum_{n=1}^{3} k_{3,n} x_{n,1} \end{aligned}$$

For the adopted values of the matrix elements, k_{ij}, see table 2. Once the *LQR* has been performed, those elements were obtained by a linear combination of the rate constants shown in table 1.

Acknowledgement: The authors wish to thank Andrea Ciliberto and Galit Lahav for their useful suggestions and the specific literary material. Marzia Sabella and Notre Dame du Cap de La Madeleine made this work possible.

References

1. Ma L, Wagner J, Rice J-J, Hu W, Levine AJ, Stlovitzky G (2005) A plausible model for the digital response of p53 to DNA damage. *Proc Natl Acad Sci USA* 40:14266-14271.

2. Geva-Zatorsky N, Rosenfeld N, Itzkovitz S, Milo R, Sigal A, Dekel E, Yarnitzky T, Liron Y, Polak P, Lahav G, Alon U (2006) Oscillations and variability in the p53 system. *Molec Syst Biol* 10.1038:1-13.

3. Shangary S, Wang S (2008) Targeting the Mdm2-p53 interaction for cancer therapy. *Clin Cancer Research* 17:5318-5324.

4. Ciliberto A, Novak B, Tyson J (2005) Steady states and oscillations in the p53/Mdm2 network. *Cell Cycle* 3:488-493.

5. Zhang T, Brazhnik P, Tyson J-J (2007) Exploring mechanisms of the DNA-damage response. *Cell Cycle* 1:85-94.

6. Harms K-L, Chen X (2005) The C terminus of p53 family proteins is a cell fate determinant. *Mol Cell Biol* 5:2014-2030.

7. Bell S, Klein C, Muller L, Hansen S, Buchner J (2002) p53 contains large unstructured regions in its native state. *J Mol Biol* 322:917-927.

8. Reich C-N, Oren M, Levine A-J (1983) Two distinct mechanisms regulate the levels of a cellular tumor antigen, p53. *Mol Cell Biol* 12:2143-2150.

9. Ventura A, Kirsch D-G, McLaughlin M-E, Tuveson D-A, Grimm J, Lintault L, Newman J, Reczek E-E, Weissleder R, Jacks T (2007) Restoration of p53 function leads to tumour regression in vivo. *Nature* 445:661-665.

10. Bates S, Phillips A-C, Clark P-A, Stott F, Peters G, Ludwig R-L, Vousden K-H (1998) $p14^{ARF}$ links the tumour suppressor RB and p53. *Nature* 395:124-125.

11. Bar-Or R-L, Maya R, Segel L-A, Alon U, Levine A-J, Oren M (2000) Generation of oscillations by the p53-Mdm2 feedback loop: a theorethical and experimental study. *Proc Natl Acad Sci USA* 21:11250-11255.

12. Lahav G, Rosenfeld N, Sigal A, Geva-Zatorsky N, Levine A-J, Elowitz M-B, Alon U (2004) Dynamics of the p53-Mdm2 feedback loop in individual cells. *Nature Genetics* – published online (www.nature.com/naturegenetics) doi 10.1038:1-4.

13. Loewer A, Lahav G (2006) Cellular conference call: external feedback affect cell-fate decision. *Cell* 124:1128-1130.

14. Batchelor E, Mock C-S, Bhan I, Loewer A, Lahav G (2008) Recurrent initiation: a mechanism for triggering p53 pulses in response to DNA damage. *Molecular Cell* 30:277-289.

15. Tsourkas A, Weissleder R (2004) Illuminating the dynamics of intracellular activity with "active" molecular reporters. *Molecular and Cell Biomechanics* 1:136-146.

16. Deguchi S, Ohashi T, Sato M (2005) Intracellular stress transmission through actin stress fiber network in adherent vascular cells. *Molecular and Cell Biomechanics* 2:205-216.

17. Zhou J, Chen J-K, Zhang Y (2007) Theoretical analysis of thermal damage in biological tissues caused by laser irradiation. *Molecular and Cell Biomechanics* 4:27-40.

18. Mooney D (2006) Materials to regulate cell fate *in vitro* and *in vivo*. *Molecular and Cell Biomechanics* 3:169-176.

19. Ardito Marretta R-M, Marino F (2007) Wing flutter suppression enhancement using a well-suited active control model. *J Aero Engng* 221:441-453.

20. Ardito Marretta R-M, Marino F, Bianchi P (2008) Computer active control of damping fluid of a racing superbike suspension scheme for road-safety improvement spin-off. *Int J Vehicle Des* 46:436-450.